Optimization Study of Rhodamine 6G Removal from Aqueous Solutions by Photocatalytic Oxidation

DOINA LUTIC[1], IGOR CRETESCU[2]*

[1]Al. I. Cuza University of Iasi, Faculty of Chemistry, 11 Carol I Blvd., 700506, Iasi, Romania

[2] Gh. Asachi Technical University of Iasi, Faculty of Chemical Engineering and Environmental Protection, 73 Mangeron Blvd., 700050, Iasi, Romania

The investigation of the optimal values of the experimental operating parameters (initial dye concentration, dose of catalyst and pH value) in the photocatalytic degradation of dye Rhodamine 6G dye from aqueous solutions was performed by following a factorial matrix plan including 18 experiments, on a catalyst prepared by incipient wet impregnation of P-25 commercial titanium dioxide with 2% WO_3. A second degree mathematical model was obtained, combining the mentioned process parameters. The results indicate an interesting, unexpected pH dependence of the decolorizing degree. An optimal photocatalyst dye dose was established to be 0.323 L^{-1}.

Keywords: experimental factorial design WO_3/P-25, Rhodamine 6G, photocatalysis

The adsorption on solids followed by the photocatalytic decolorizing and mineralization of stable, pollutant dyes is a convenient method for wastewaters treatment. These wastewaters are usually produced by textile industry and biological analysis. There are similarities between the photocatalytic reactions and the heterogeneous catalysis, consisting in an organic species adsorption on a solid, followed by the oxidation on the surface by active oxygenated species. The photoactive solids are semiconductive oxides and can capture the energy of photons and use it for the reaction activation. The photocatalyst must therefore be a good adsorbent and ensure the oxygenated species to locate on the surface, in the close nearby of reducing species. An efficient photocatalyst must therefore offer a high specific surface area. An open pore structure of the catalyst also leads to an increase of the number of adsorption sites. The photocatalytic reactions usually occur at temperature values close to ambient; therefore, the photoreactions are "greener", due to the energy saving for the reaction activation and to the minimization of secondary reactions often occurring in the heterogeneous processes activated by heat [1-4].

Titanium dioxide in the form of anatase is the most common oxide used as a photocatalyst. The anatase form of TiO_2 has a bandgap wide of 3.2 eV, enabling to capture energy from UV and solar light, which is largely available, green and costless. When an electron is promoted between the valence band and the conduction band, an electron-hole pair is generated. The holes react with water forming $HO^{\cdot}$ radicals and protons, while the electrons react with oxygen give $^{\cdot}O_2^-$ radical-ion. The $^{\cdot}O_2^-$ species combines with two protons and one electron generating hydrogen peroxide and it decomposes in hydroxyl radicals and hydroxyl ions in the presence of electrons. Thus, in both so-called hole and electron pathways described, hydroxyl radicals $HO^{\cdot}$ are formed. This is the key-species involved in the photocatalytic oxidation. The photocatalytic reaction occurs on the catalyst surface between the adsorbed organic species and the $HO^{\cdot}$ radicals [5]. Numerous studies indicate a synergetic effect of energy capturing when two different species of semiconducting oxides are associated in the same solid, due to the decrease of the probability of electron-hole recombination [6].

Rhodamine 6G (R_6G) is an organic dye, soluble in water and giving easily observable color even with the naked eye, also at low concentrations of some ppm. It makes R_6G a good tracer to prove the transport direction of underground water courses. It also finds applications in the fluorescence microscopy and spectroscopy), as well as in the biochemical analysis ELISA, to detect the presence of an antigen, in a liquid or wet sample. The persistent color of R_6G needs its decolorizing or eventually mineralization in order to remove the embarrassing color from water [7].

In our work, we performed a parametric study by following an experimental matrix allowing to elaborate a mathematical model able to describe the system behaviour, in terms of optimal reaction conditions for the photodegradation of Rhodamin 6G (R_6G) dye. The catalyst was the commercial P-25 titania doped with 2% WO_3. The investigated parameters on the photodegradation degree were the initial dye concentration, the photocatalyst dose and the *p*H value.

Experimental part

A commercial sample of titanium dioxide, P-25 from Degussa was used for the preparation of the photocatalytic active material, by doping with WO_3. The doping procedure was performed by the incipient impregnation technique (IWI), by pouring 3 mL solution of sodium wolframate dissolved in water on a sample of 1 g P-25. The amount of impregnating salt was calculated to reach a 2% mole ratio of WO_3 to TiO_2. The activation of the sample was performed by slow heating ($2^{o}min^{-1}$) at 723K, maintaining for 4 h and spontaneous cooling afterwards. The investigation of the solids porous structure was performed by BET nitrogen adsorption. The photocatalytic degradation was performed in a 300 mL glass reactor (fig. 1), equipped with a central quartz tube hosting an Osram UV-A lamp of 9W (wavelength range 350-400 nm, maximum at 370 nm), used for the UV irradiation of the dye solution. A magnetic

* *email: icre@tuiasi.ro*

rod placed at the reactor bottom was used for the stirring. The samples of dye of 250 mL were prepared using ultra-pure water. The *p*H value was measured by a Hanna HI 991003 pH-meter and set to the chosen value by adding in small drops sulfuric acid 0.1 M or Sodium hydroxide 0.1 M. In the dye solution, the photocatalyst powder was then added and the suspension was magnetically stirred for 30 minutes in dark, to establish the adsorption/desorption equilibrium. Finally, the lamp was turned on; this moment is considered the beginning of the photocatalytic reaction and labeled as zero-time. At specific time intervals, samples of 5 mL suspension were taken from the reaction vessel, filtered immediately through a 0.2μm filter for catalyst separation and analyzed to determine the remaining dye concentration.

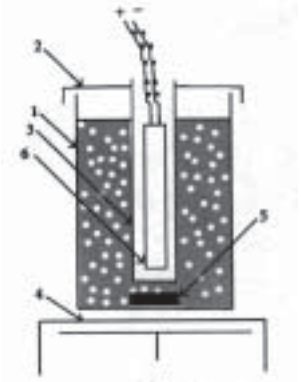

Fig. 1. The photocatalysis experimental setup [6]
1-glass reactor, 2-opaque lid, 3-quartz tube, 4- magnetic stirrer, 5-magnetic range, 6-UV lamp

All the experiments were run at ambient temperatures, comprised between 295-297 K. The influence of the temperature on the reaction is not interesting, since the activation energy in a photocatalytic reaction comes from irradiation and the eventual secondary heating can be neglected. The dye concentration was measured using UV–Vis spectroscopy on a Shimadzu UV-1700 spectro-photometer. The UV-Vis spectrum of R_6G displays a net maximum at 526 nm. The calibration performed to check the extinction – concentration linearity showed an excellent linearity up to 10 ppm dye. The samples with higher concentrations were diluted before measuring the extinction at the requested ratios in order to stay in the linearity range for the colorimetric measurements.

The decolorizing of the dye solution was taken as a measure of the degradation efficiency. The dye removal degree was calculated using the equation (1):

$$Dye\_removal(\%) = \frac{C_0 - C_t}{C_0} \times 100 \qquad (1)$$

where C_0 and C_t are the initial and t - time concentrations of R_6G

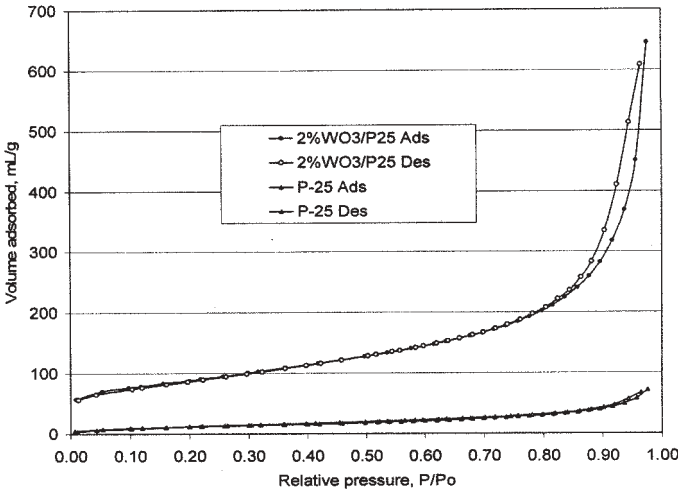

Fig. 2. BET isotherm of the sample 2%WO_3/P-25 compared to P-25

Results and discussions

Characterization of the porous photocatalyst

The BET analysis of the sample 2%WO_3/P-25 showed a solid with a relatively high surface area (271 m^2g^{-1}), compared to the parent sample having only 46 m^2g^{-1}. The BET isotherm has a hysteresis loop with a shape intermediate between H_3 and H_4, indicating the formation of slit narrow pores between the particles. The dramatic increase of the specific surface area is due to the formation of an important secondary porosity of the sample given by interparticle free space, as suggested by the position of the steep increase of the adsorbed amount of nitrogen (around $p / p_o = 0.9$) and by the narrow hysteresis loop. The re-arrangement of the particles is due to both thermal procedure as well as to the presence of the dopant, which acts as a binder for the small particles of P-25. The same behaviour has been reported by Zhang et al [8] and Xiang et al. [9].

Decolorizing evolution

The UV-Vis spectrum of Rhodamine 6G dye and the dye chemical structure is displayed in figure 3. The narrow band at 523 nm from the visible region of the spectrum is due to the chromophore (the azo group), while the bands from 275 and 246 nm in the UV region are due to the aromatic part of the molecule [10, 11].

By following the evolution of the UV-Vis spectra, the progressive decrease of the peak from 523 nm highlighting the decolorizing is accompanied by the decrease of bands from the UV region, indicating that the intermediate aromatic products are further mineralized. The band in the spectrum at around 215 nm could not be precisely

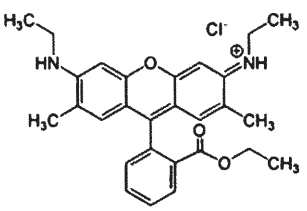

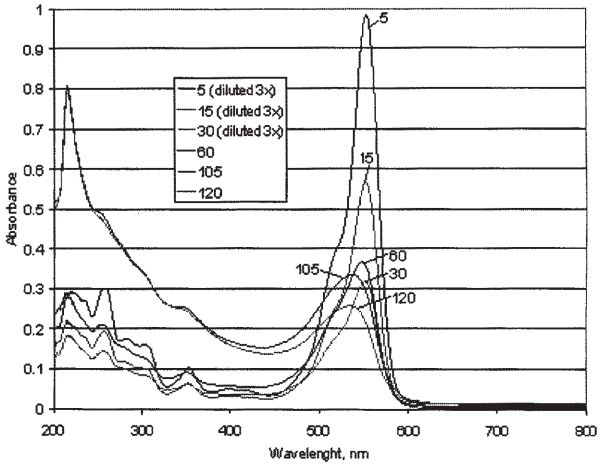

Fig. 3. Rhodamine 6G chemical structure and UV-Vis spectra of evolution in time (experimental conditions: 30 ppm dye, 0.3 g L^{-1} catalyst, *p*H 5)

N	Dye concentration, ppm (x_1)	Catalyst concn., g/L (x_2)	pH (x_3)	Reduced values (x_1)	(x_2)	(x_3)	System response (Y_1)120	(Y_2)60
1	50	0.5	7.5	+1	+1	+1	93.93	85.41
2	10	0.5	7.5	-1	+1	+1	96.32	95.39
3	50	0.1	7.5	+1	-1	+1	73.89	69.74
4	10	0.1	7.5	-1	-1	+1	94.13	92.89
5	30	0.3	7.5	0	0	+1	93.83	83.25
6	30	0.3	4.5	0	0	-1	87.36	75.85
7	50	0.5	4.5	+1	+1	-1	74.30	69.16
8	10	0.5	4.5	-1	+1	-1	96.52	95.51
9	50	0.1	4.5	+1	-1	-1	48.21	35.41
10	10	0.1	4.5	-1	-1	-1	86.10	80.33
11	54.3	0.3	6	$\sqrt{2}$	0	0	86.28	81.93
12	5.7	0.3	6	$-\sqrt{2}$	0	0	88.80	91.69
13	30	0.543	6	0	$\sqrt{2}$	0	91.99	89.63
14	30	0.057	6	0	$-\sqrt{2}$	0	51.76	48.28
15	30	0.3	7.8225	0	0	$\sqrt{2}$	88.99	75.58
16	30	0.3	4.1775	0	0	$-\sqrt{2}$	96.18	71.48
17	30	0.3	6	0	0	0	94.51	76.66
18	30	0.3	6	0	0	0	95.08	76.10

(Y_2)-corresponding to 60 min, respectively (Y_1)- corresponding to 120 (T = 295-297 K)

Table 1
EXPERIMENTAL MATRIX DESIGN AND SYSTEM RESPONSES FOR THE OPTIMIZATION OF R_6G PHOTODEGRADATION

assigned, but seems to be due to the presence of carbonyl groups in acid, ester and amide species [12].

Factorial Design of the Parameters Influencing the Photoreaction

Experimental matrix design

From the high number of possible parameters influencing the photocatalytic reaction, three were considered for the present study, namely: the photocatalyst concentration, the *p*H value and the initial dye concentration. These are considered to be the most important ones, since we assumed the reaction runs under isothermal conditions of reaction at room temperature. For potentially applicative reasons, the time duration of a typical run was limited to 120 min. A longer run under artificial UV irradiation means an energy consummation too high to remain economically acceptable.

Blank experiments using the same reagents with no irradiation and the irradiation of the solution in the same set of conditions without adding the solid photocatalyst, reached a conversion degree of only some percents, proving that the use of both UV light and of the photocatalyst were necessary.

Obtaining the empirical model equations for the formulation of the system response to the input controllable variables is the main step in a Response Surface Methodology-based (RSM) optimization process. RSM is an usual optimization approach, allowing to locate an extreme point on the surface of the model response, i.e. a set of parameters values in which the optimum system response (usually a maximum) is observed [13-17]. The mostly used models in RSM are the polynomial regression equations with the general form [18]:

$$Y = b_0 + \sum b_i x_i + \sum b_{ii} x_i^2 + \sum b_{ij} x_i x_j \quad (2)$$

where:

Y is the calculated system response (the dye removal efficiency, in our case);

x_i: the factors influencing the system response (the input variables – the catalyst and the initial dye concentrations and the *p*H value);

b_0, b_i, b_{ii}, b_{ij}: regression coefficients

In the RSM, the factors are usually scaled up to coded levels in order to facilitate the calculations. Basically, the values of each factor assumes three different coded levels ranging from low (-1) to medium (0) and high (+1). In addition, depending on the type of the experimental design, the axial levels ($\pm\alpha$) can be also considered. The effective values of the parameters from the experimental matrix were chosen according to literature at extreme reasonable values of the fore-mentioned parameters adequately. The experiments were run at the parameters values listed in table 1. The system responses (Y_1 and Y_2) were the decolorizing degrees at time durations of 60 and 120 minutes from the beginning of the irradiation.

Response surface modeling

The success in developing the polynomial model requires an appropriate experimental design, in order to obtain efficient information. The preference for the central compositional design (CCD) comes from the easiness to use the sequential experimentation. In contrast to the conventional methods of experimentation when the factors are varied one by one, the CCD supposes the simultaneous variation of the factors. This approach brings advantages for highlighting the interaction effects between different factors, allowing to decrease the number of experimental runs, shortening thus the number of experimental runs so the decrease of the experimental duration, reagents amounts and overall expenses.

The regression coefficients for the empirical polynomial model were calculated by using the least squares (OLS) method. The estimations of the regression coefficients can be written as follows [8-13]:

$$b = (x^T x) x^T Y \quad (3)$$

where:

b: the vector of the regression coefficients;

x: the design matrix for the input variables;

Y: the column vector of experimental response

In this work, the CCD of orthogonal type produces a polynomial regression model and illustrates a functional relation between the dye decolorizing efficiency the three

experimental factors. The coefficients of the polynomial regression equations computed by the OLS-method led to the following polynomial models:

$$Y_1 = - 277x_2^2 – 1.72x_1 + 194\ x_2 - 3.3\ x_3 + 0.829\ x_1x_2 + 0.185\ x_1x_3 + 89.2$$

$$Y_2 = - 84.3\ x_2^2 – 1.91\ x_1 + 87.5\ x_2 - 2.67\ x_3 + 0.804\ x_1x_2 + 0.184\ x_1x_3 + 92.3$$

Both models resulting from the experimental matrix design are adequate (R_{Sq} = 88.7 and 94.1 % respectively), since the maximum abatement between the experimental and calculated values were 11.3 and 5.9 %, respectively.

Based on the statistically validated model, the graphical representations of the response surface were plotted. The response surface plots and their associated contour-lines maps are illustrated in figures 4-7.

Aiming to determine the extreme points (points of maximum, according to the response surfaces and the section profiles displayed in the outline plots), the first order derivatives of the response function in relation to each variable (x_1, x_2, x_3) were calculated and equalized to 0. Two first degree sets of equations result as follows:

$$Y_1: \quad \frac{\partial Y_1}{\partial x_1} = 0.829x_2 + 0.185x_3 – 1.72 = 0 \qquad (4)$$

$$= 0.829x_1 - 554x_2 + 194 = 0$$

$$= 0.185x_1 – 3.3 = 0$$

$$Y_2: \quad = 0.804x_2 + 0.184x_3 – 1.91 = 0 \qquad (5)$$

$$= 0.804x_1 - 2\times84.3x_2 + 87.5 = 0$$

$$= 0.184x_1 – 2.67 = 0$$

The solutions of these equations in terms of real values for the variables are displayed in table 2.

The values from table 2 indicate that the optimal concentration for both functions Y_1 and Y_2 is situated between 14-18 ppm of dye. It is worth to note that for longer time-on-stream, the optimum increases slowly, indicating that the degradation process is continued, leading to the more advanced degradation degree of dye in time. In the case of the *p*H value, the highest *p*H in the investigated range had been found to be optimum for the Y_1, while Y_2 function maximum appeared at even higher *p*H values. This solution is outside the considered pH range, taking into consideration in the experimental matrix design. In this case, the optimum value was chosen to be the high limit from the *p*H range [19] considered in experimental matrix design.

In order to obtain a further confirmation of the model validity, due to the fore-mentioned situation of the optimum by or even above the considered limits from the range, a detailed *p*H dependence of the reaction evolution was

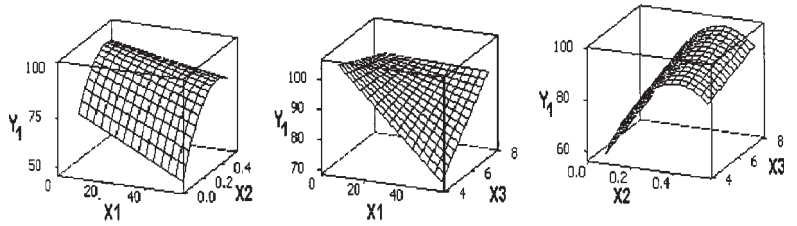

Fig. 4. Response surfaces for the function Y_1 depending on the variables x_1-x_2 (at x_3 = 6); x_1-x_3 (at x_2 = 0.3) and x_2 - x_3 (at x_1 = 30)

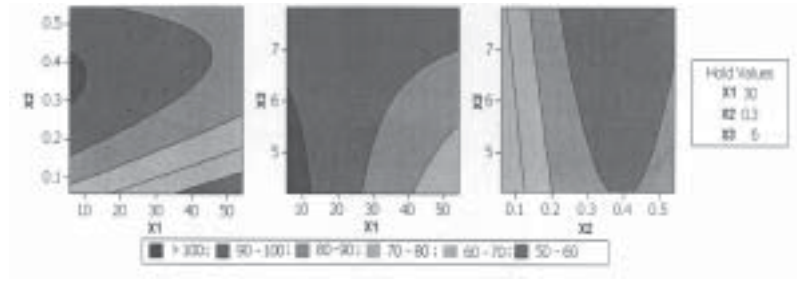

Fig. 5. Response surface plot and contour-lines map for the response function Y_1 depending on sets of two variables, while holding the third at the mentioned value

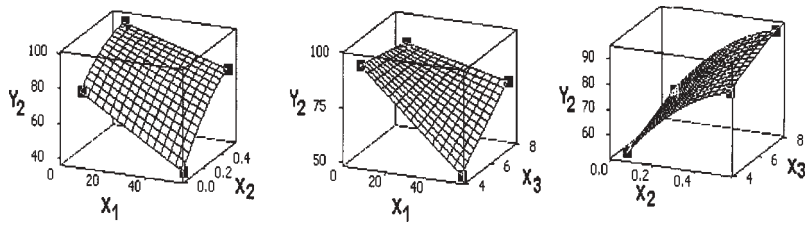

Fig.6. Response surfaces for the function Y_2 depending on the variables x_1-x_2 (at x_3 = 6); x_1-x_3 (at x_2 = 0.3) and x_2 - x_3 (at x_1 = 30)

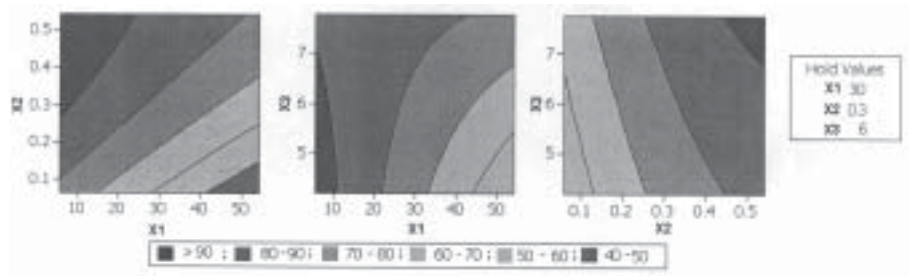

Fig.7. Response surface plot and contour-lines map for the response function Y_2 depending on sets of two variables, while holding the third at the mentioned value

Response/process variables	x_1	x_2	x_3
$Y_1 = 97.058$	17.837	0.323	7.846
$Y_2 = 93.747$	14.510	0.588	12.950

Table 2
OPTIMAL VALUES FOR THE PROCESS PARAMETER CORRESPONDING TO THE MODELS

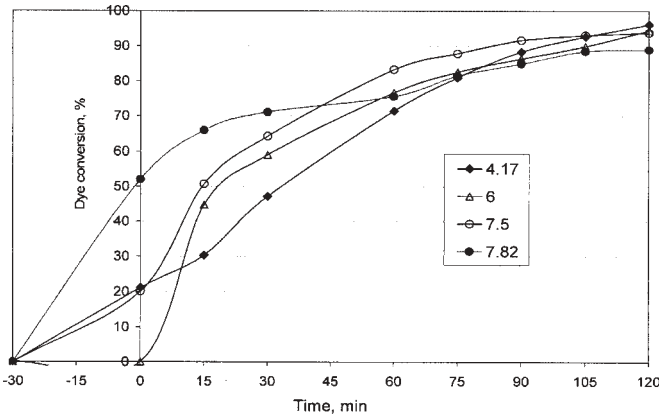

Fig. 8. pH dependence of the R_6G conversion

performed at an initial dye concentration of 30 ppm (this value being considered reasonable for eventual practical applications of the reaction) and a photocatalyst dose of 0.3 g/L solution. The results are displayed in figure 8.

The results obtained confirm that the high values of the *p*H are very favorable on the decolorizing of R_6G, since at both 7.5 and 7.82 the conversion is very high. An interesting aspect is also that these alkaline *p*H values prove to be very favorable on the dye adsorption, since at *p*H = 7.82, half of the dye from the solution is adsorbed during the 30 min allocated to the adsorption equilibrium, then it is progressively photo-decomposed to an extent of 90% in 120 min. It is surprising that this detailed series of experiments show that also the acid *p*H of 4.17 ensures excellent conditions for the dye decomposition. This behavior can be explained in terms of adsorption of the dye on the surface. The alkaline or acid pH determine the strong ionization of the dye and in this form, the dye attaches easily on the photocatalyst surface by interacting with the electron-rich or hole-rich sites.

Conclusions

The decolorizing of Rhodamine 6G dye solutions with concentrations between 5.4-57.3 ppm was performed in the presence of P-25 titania doped with 2%WO_3. A series of 18 experiments were made in the framework of a factorial design aiming to develop a mathematical model able to describe the contribution of three parameters (initial concentration of the dye, photocatalyst dose and pH value) on the decolorizing degree. The optimal values according to the model were situated within the considered range for the first two parameters (dye concentration 18 ppm, catalyst concentration 0.58 g L^{-1} after 120 min) and at the highest tested value for the *p*H. The detailed study on the *p*H influence on the process indicated that indeed the high *p*H is favorable for the dye adsorption and reaction, but also the low *p*H values favors the dye decomposition.

Acknowledgements: The authors are grateful for the partial support of this work by the Bilateral Research Grant Romania-Greece no. 576/ 2012.

References

1. CHONG M. N., JIN B., CHOW C. W.K., SAINT C., Water Res., **44**, 2010, p. 2997.
2. DI PAOLA A., GARCÍA-LÓPEZ E., MARCÌ G., PALMISANO L., J. Haz. Mater., **211-212**, 2012, p. 3.
3. OLLER I., MALATO S., SÁNCHEZ-PÉREZ J.A., Sci. Total Envir.,. 409, 2011, 2011, p. 4141.
4. HASHIMOTO K., IRIE H., FUJISHIMA A., AAPPS Bulletin, **17**, nr. 6, 2007, p. 12.
5. T. AARTHI, T. and MADRAS, G., Ind. Eng. Chem. Res., **46,** 2007**,** p. 7.
6. YU, C, YU, J. C., ZHOU, W, YANG, K., Catal. Lett. **140**, 2010, p. 172.
7. LUTIC, D., COROMELCI-PASTRAVANU, C., CRETESCU I.**,** POULIOS, I., STAN, C.D., Int. J. Photoenergy, Article ID 475131, 2012 (doi:10.1155/ 2012/475131)
8. ZHANG, M., YU, X., LU, D., YANG, J., Nanoscale Research Letters, **8,** 2013, p. 543
9. XIANG, L. J., NATHAN-WALLESER, T. International Journal of Material Science (IJMSCI), **3**, nr. 3, 2013, p. 104.
10. RAMIREZ, J.H., COSTA, C.A., MADEIRA, L.M., MATA, G., VICENTE, M.A., ROJAS-CERVANTES, M.L., LOPEZ-PEINADO, A.J., MARTIN-ARANDA, R.M., Appl. Catal. B: Envir. **71,** 2007, p. 44
11. DÜKKANCÝ, M., GÜDÜZ, G., YÝLMAZ, S., YAMAN, Y.C., PRIKHOD'KO, R.V., STOLYAROVA I.V., Appl. Catal. B: Envir. **95,** 2010, p.270.
12. POPL , M., FÄHNRICH, J., TATAR, V. (editors), Chromatographic Analysis of Alkaloids, Marcel Dekker, 1990, p. 50 (https:// books.google.ro/books?id=RTCDsHbLH2gC&pg= PA50&lpg= PA50&dq=uv+SPECTRA+215+nm&source=bl&ots= qTk2SDfQU&sig =RCwBxaua-PdZq_ vEpolPopw-VeI&hl=en&sa=X&ei= VGHHVK2oL KezygO8lIHoBg&ved= 0CDEQ6AEwBQ#v= onepage&q= uv%20 SPECTRA%20215%20nm&ffalse)
13. CARAIMAN, P., POHONTU, C., SOREANU, G., MACOVEANU, M., CRETESCU, I., Envir. Eng. Manag. J., **11** nr. 2, 2012, p. 271.
14. POHONTU C., CRETESCU, I., SECULA, M.S., MACOVEANU, M., Envir. Eng. Manag. J., **10,** nr. 3, 2011, p. 327.
15. COJOCARU, C., CRETU, V.C., PREDA, C., MACOVEANU, M., CRETESCU, I., J. Envir. Prot. Ecol., **11,** nr. 2, 2010, p. 643.
16. SECULA, M., SUDITU, G., POULIOS, I., COJOCARU, C., CRETESCU, I., Chem. Eng. J., **141**, nr. 1-3, 2008, p.18.
17. SUMAN, I., COJOCARU, C., CRETESCU, I., DUCA, GH., MALINA, J., COVALIOV, V., Rev. Chim.(Bucharest), **58**, no. 11, 2007, p. 1134.
18**.** CRETESCU, I., SAVIN, AL., CIMPEANU, C., BUCUR, R.D., HARJA, M., J. Food Agric. Envir., **11**, nr. 1, 2013, p. 221.
19. CRETESCU, I., MACOVEANU, M., Rev. Chim.(Bucharest), **49**, no. 10, 1998, p. 682.

Manuscript received: 7.07.2014